Tuning functional properties by plastic deformation

New Journal of Physics
The open-access journal for physics

Tuning functional properties by plastic deformation

A R Kwon[1,2], V Neu[1], V Matias[3], J Hänisch[1,3], R Hühne[1], J Freudenberger[1], B Holzapfel[1], L Schultz[1,2] and S Fähler[1,4]

[1] IFW Dresden, Institute for Metallic Materials, PO Box 270116, 01171 Dresden, Germany

[2] Department of Mechanical Engineering, Institute for Materials Science, Dresden University of Technology, 01062 Dresden, Germany

[3] Superconductivity Technology Center, Los Alamos National Laboratory, Los Alamos, NM 87545, USA

E-mail: s.faehler@ifw-dresden.de

New Journal of Physics **11** (2009) 083013 (10pp)
Received 28 April 2009
Published 13 August 2009
Online at http://www.njp.org/
doi:10.1088/1367-2630/11/8/083013

Abstract. It is well known that a variation of lattice constants can strongly influence the functional properties of materials. Lattice constants can be influenced by external forces; however, most experiments are limited to hydrostatic pressure or biaxial stress. Here, we present an experimental approach that imposes a large uniaxial strain on epitaxially grown films in order to tune their functional properties. A substrate made of a ductile metal alloy covered with a biaxially oriented MgO layer is used as a template for growth of epitaxial films. By applying an external plastic strain, we break the symmetry within the substrate plane compared to the as-deposited state. The consequences of 2% plastic strain are examined for an epitaxial hard magnetic $Nd_2Fe_{14}B$ film and are found to result in an elliptical distortion of the in-plane anisotropy below the spin-reorientation temperature. Our approach is a versatile method to study the influence of large plastic strain on various materials, as the MgO(001) layer used is a common substrate for epitaxial growth.

[4] Author to whom any correspondence should be addressed.

Contents

1. Introduction

Lattice constants determine most of the functional properties of solid matter; in particular their ferroelectric [1], (magneto- [2]) resistance [3], superconducting [4], martensitic [5], multiferroic [6], magnetocaloric [7]–[9] and elastocaloric [10] properties. Materials, however, typically exhibit only one set of lattice parameters at a given temperature. Wherever possible, the ability to control lattice parameters helps us significantly to understand the origin of the relevant interactions. In addition, a significant improvement of an effect [1, 2], an increased application temperature [5] or even complete new functionalities [7], [10]–[12] are sometimes obtained. The easiest approach to tune lattice constants is to replace some atoms by atoms of different sizes. This, however, may also modify the electronic structure; therefore non-equilibrium methods varying only the lattice parameters are favorable. For bulk materials, hydrostatic pressure can often be used [7]–[10], [13] to vary the lattice constants. In contrast to this three-dimensional compression, thin films allow a quasi-two-dimensional control of lattice parameters, since the in-plane lattice parameters can be constrained by the substrate [1], [3]–[6]. Very large strain is possible in epitaxial films of a few unit cells [14, 15] and multilayers. The finite number of atomic layers, however, makes these ultrathin films a new class of materials, dominated by their interface and surface. In order to understand bulk properties, thicker films are more favorable. With a film thickness of some hundreds of unit cells, the influence of the surface can be neglected, allowing a better comparison with bulk properties. Also, thin films often withstand a larger ultimate strain than bulk material [16, 17]. Thus large elastic deformation is feasible in thin films.

Several methods to introduce strain in several hundred nm thick magnetic films are commonly used: differences in thermal expansion coefficient [5] and lattice mismatch [18] of film and substrate, reversible strain by piezoelectric substrates [3, 19], and substrate expansion by hydrogen injection [20]. With these methods, a biaxial strain below 0.6% can be reached. In this paper, we demonstrate an approach to introduce uniaxial strain up to 2%. Ni-based transition metal Hastelloy [21], which has a high ductility and no ferromagnetic order, is used as a substrate. Substrates and films were strained in tension by a mechanical testing machine (figure 1). Contrary to the other approaches, this uniaxial strain breaks the in-plane symmetry of the thin film. Recently, a similar approach has been shown to enhance the giant magnetoresistance (GMR) effect in polycrystalline Co/Cu multilayers grown on plastic substrates [2]. However, functionally epitaxial films are most simple in order to investigate

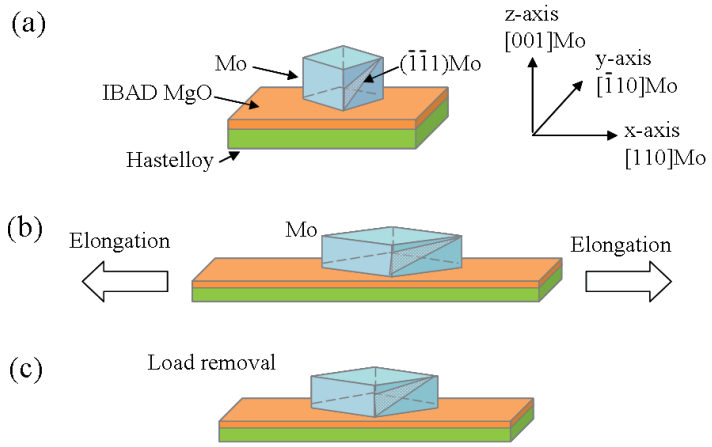

Figure 1. Sketch of strain condition of the films–substrate-composite. (a) The geometry after deposition. On a ductile Hastelloy substrate (green) a biaxially textured MgO buffer was grown by IBAD (orange). On top of this, an epitaxial Mo buffer (blue) is used to mediate the epitaxial growth of $Nd_2Fe_{14}B$ (not shown). The trihedron shows the orientations used for the measurements of the lattice constants and in particular the orientation of the (111) plane is marked within the Mo unit cell. (b) The substrate and film during elongation. (c) The substrate and film after being plastically strained.

the symmetry breaking effect by uniaxial strain. To allow this, we deposited a biaxially textured MgO(001) buffer by ion-beam-assisted deposition (IBAD) on top of the polycrystalline Hastelloy substrate [22]. The MgO(001) surface is a suitable template for the epitaxial growth of a broad range of materials and this substrate/buffer combination allows a broad range of growth temperatures. Thus, our approach is applicable to a large variety of functional materials.

For a proof of concept, $Nd_2Fe_{14}B$ is selected as the functional material giving the best hard magnetic properties to date [23]. In the form of thin films, highly textured [24]–[26] and epitaxial films [27, 28] of this material with optimized properties are available for magnetic microelectromechanical systems and magnetic data storage. Unlike in soft magnetic materials, the effect of strain on the overall magnetic anisotropy is usually considered to play a minor role in $Nd_2Fe_{14}B$ due to its large magnetocrystalline anisotropy. Contrary to a simple uniaxial magnet, $Nd_2Fe_{14}B$, however, exhibits a spin reorientation below 135 K, which originates from the competition of the Nd and Fe sublattice anisotropies and manifests itself in a sign change of the first anisotropy constant K_1 [29]. This suggests that in this temperature regime a significant variation of the intrinsic magnetic properties by strain should be possible. For bulk materials, an external control of lattice parameters has been realized by hydrostatic pressure and hydrogen loading [30]. In addition, uniaxial compression of polycrystalline samples has been performed, revealing ensemble averaged magnetostrictive anisotropy constants [30, 31]. For bulk materials, however, a measurement of the directional dependency is hampered by the poor availability of single crystals and their high brittleness. In addition, several studies focus on spontaneous magnetostriction. Temperature-dependent changes of the unit cell [32, 33] are intended to reveal information about the magnetic interactions between the 64 atoms in this unit cell.

2. Experimental

To obtain epitaxial growth on the polycrystalline Hastelloy (Hastelloy C-276), a biaxially oriented MgO(001) layer was deposited using IBAD [22]. A 10-nm-thick IBAD MgO was deposited at room temperature with an ion beam current density of 0.8 mA cm^{-2} and ion energy of 1 keV. For improving the texture, a 200 nm-thick homoepitaxial MgO layer was deposited at approximately 600 °C, which has an in-plane full-width at half-maximum of 4°. In a next step, a 50 nm-thick Mo layer and a 300 nm-thick Nd–Fe–B film were deposited at 450 °C analogous to the preparation of this film architecture on a single-crystal MgO(001) substrate [34]. Film deposition by pulsed laser deposition in ultra high vacuum was described in detail previously [35]. In order to protect the $Nd_2Fe_{14}B$ from oxidation, a 30 nm Mo protection layer was deposited on top of the film after cooling below 250 °C. Integral magnetic properties were determined at varying temperatures using a vibrating sample magnetometer (Quantum Design PPMS). The crystal structure was analyzed by x-ray diffraction (XRD) in a 4-circle Philips X'Pert diffractometer using Cu–K_α. In addition, the lattice parameters perpendicular to the substrate direction were measured in Bragg Brentano geometry using Co–K_α radiation. Mechanical testing was carried out with a conventional tensile test machine (Instron 8562).

3. Results and discussions

3.1. Plastic deformation

Figure 1 shows a sketch of the strain condition for the film–substrate composite. Uniaxial stress was applied using a tensile test machine after film deposition. All the measurements were done after removing uniaxial load from the sample; therefore only plastic deformation remains on the substrate and both elastic deformation and plastic deformation remain on the film during the measurements. Although Hastelloy can withstand a plastic strain of up to 30%, the applied plastic strain was limited in our experiments to 2% as a further increase results in cracks in the Nd–Fe–B layers, which leads to an inaccurate stress control.

According to pole figure measurements on as-deposited films (figure 2(a)), Mo grows epitaxially on IBAD MgO(001) with the epitaxial relation: (001)⟨110⟩Mo||(001)⟨100⟩MgO as known from the growth on single-crystal substrates [34]. The (105) pole figure of $Nd_2Fe_{14}B$ contains 12 peaks, suggesting the existence of three equivalent orientations of the tetragonal basal plane on Mo(001). This is different from the growth on MgO(001) single crystals, where only one single orientation is observed [34]. Although the overall composition is the same, a high intensity of the Nd(004) appears in the film on IBAD MgO/Hastelloy. Since the hexagonal symmetry of Nd differs from the cubic MgO buffer, we suggest that the growth of Nd nucleates at the small angle grain boundaries present within the IBAD buffer, but not in a single crystal. The symmetry of the highly oriented hexagonal Nd interlayer observed on the IBAD buffer can explain the three equivalent in-plane orientations for the Nd–Fe–B growth. However, like in the case of an MgO single-crystal substrate, the *c*-axis is perpendicular to the film plane. Although a single in-plane orientation, as obtained in MgO(001) single crystals, should be possible by an optimized Nd poor composition, we choose the sample with the three orientations since this averages out the in-plane anisotropy of the tetragonal unit cell because this allowed a direct comparison of the strain-induced anisotropy with magnetocrystalline anisotropy.

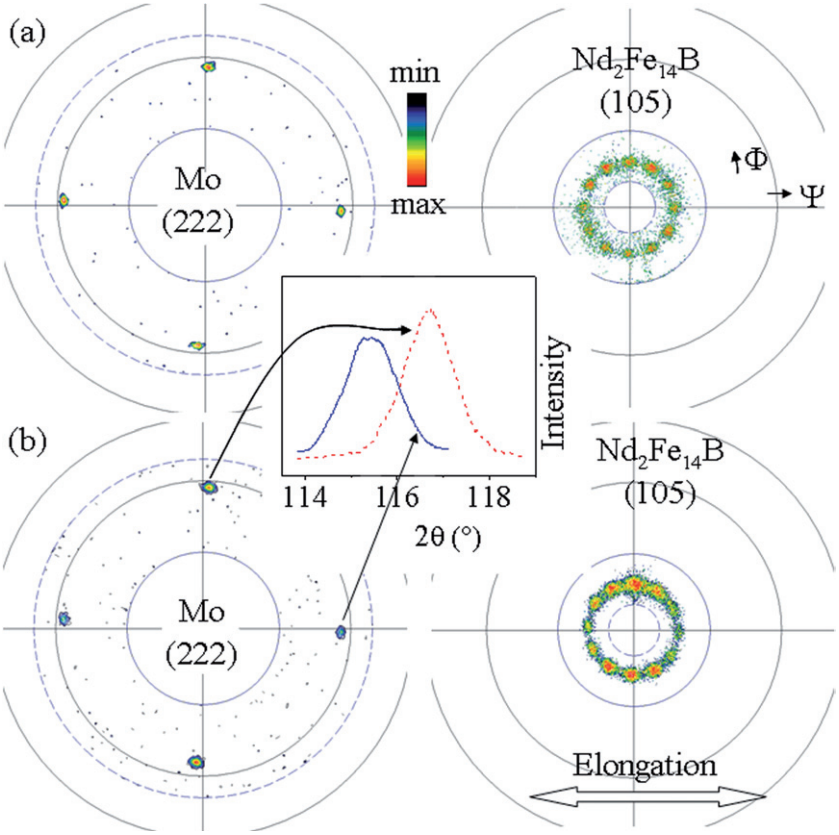

Figure 2. XRD measurements of the samples before and after being plastically strained. (222) pole figure of Mo and (105) pole figure of $Nd_2Fe_{14}B$ are shown (a) before deformation and (b) after deformation. Continuous lines mark $\Psi = 30°$, 60° and 90°. The inset shows $\theta - 2\theta$ measurements obtained with a three-circle diffractometer at two different Mo pole positions in order to extract the lattice constants.

Pole figures after 2% plastic strain (figure 2(b)) exhibit an additional twofold modulation of the peak intensity for the Mo as well as for the $Nd_2Fe_{14}B$ layer. This originates from the deformed unit cells, which do not fulfill the selected $\theta - 2\theta$ condition exactly any more. A direct measurement of the deformation of the Nd–Fe–B unit cell is not possible since the (105) pole figure is the only one not being overlapped by significant x-ray intensity from the other phases. In addition, the (105) pole figure on average shows low x-ray intensities and the angle ψ is low causing a little sensitivity for the in-plane lattice parameters, hiding a direct measurement of the deformed $Nd_2Fe_{14}B$ unit cell.

$\theta - 2\theta$ measurements on different Mo reflections, however, allow the elastic strain within the film to be quantified. The (002) lattice spacing perpendicular to the substrate and the {222} lattice spacings, which possess a projection parallel or perpendicular to the elongation direction (shown in figure 1), have been measured before and after the sample was strained. From these, the distortion ε in all three directions can be calculated. In the as-deposited state, the cubic to tetragonal distortion is below 0.28%, which may be due to growth stresses, giving an offset for this approach. In figure 3, $\theta - 2\theta$ measurements on the different {222} reflections of the Mo

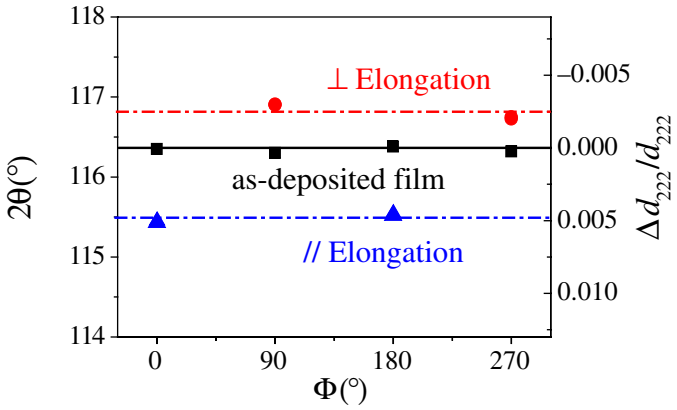

Figure 3. Elastic deformation of the Mo buffer before and after being plastically strained. Reflex positions (2θ) of Mo {222} planes and corresponding relative variation of lattice constants ($\Delta d_{222}/d_{222}$) are shown for different angles Φ (see figure 2). While there is no difference for the unstrained film (■), after elongation the lattice constants parallel to the elongation direction (▲) are increased and those perpendicular to this direction are decreased (●). Experimental errors are within the symbol size.

are shown. The Mo {222} planes in the as-deposited film have $2\theta = 116.38^\circ \pm 0.01^\circ$ in all four directions. After deformation, the lattice constants differ significantly. As shown in the inset of figure 2, $2\theta = 116.80^\circ \pm 0.04^\circ$ perpendicular and $2\theta = 115.48^\circ \pm 0.03^\circ$ parallel to the axis of the applied strain were observed after the deformation.

From this the strain on Mo {222} planes is calculated. As these planes have a certain angle to the substrate plane, additionally the out-of-plane lattice parameters are used to calculate the in-plane strain as follows. The epitaxial growth of the Mo unit cell allows use of the lattice spacing $d_{\bar{2}\bar{2}2}$ (parallel to the elongation), $d_{2\bar{2}2}$ (perpendicular to the elongation) and d_{002} (perpendicular to the substrate) to calculate the lattice constants d_{110} (parallel to the elongation) and $d_{1\bar{1}0}$ (perpendicular to the elongation). By elementary geometry, the d spacing of each {110} plane is obtained by

$$d_{110} = \frac{d_{111}}{\sqrt{1 - (d_{111}/d_{001})^2}} \tag{1}$$

Based on (1), the values of ε_x, ε_y and ε_z are

$$\begin{aligned} \varepsilon_x &= \varepsilon_{\|\text{elongation}} = \frac{\Delta d_{110}}{d_{110}} = +0.0081 \pm 0.0001, \\ \varepsilon_y &= \varepsilon_{\perp\text{elongation}} = \frac{\Delta d_{\bar{1}10}}{d_{\bar{1}10}} = -0.0026 \pm 0.0001, \\ \varepsilon_z &= \varepsilon_{\text{out-of-plane}} = \frac{\Delta d_{001}}{d_{001}} = -0.0018. \end{aligned} \tag{2}$$

Since these measurements probe the lattice constants, they give the remaining elastic deformation of the film. The measured elastic strain of 0.8% along the elongation direction is lower compared with the 2% plastic deformation of the Hastelloy substrate, suggesting that a partial plastic deformation also occurred with the Mo buffer. The volume of the Mo unit

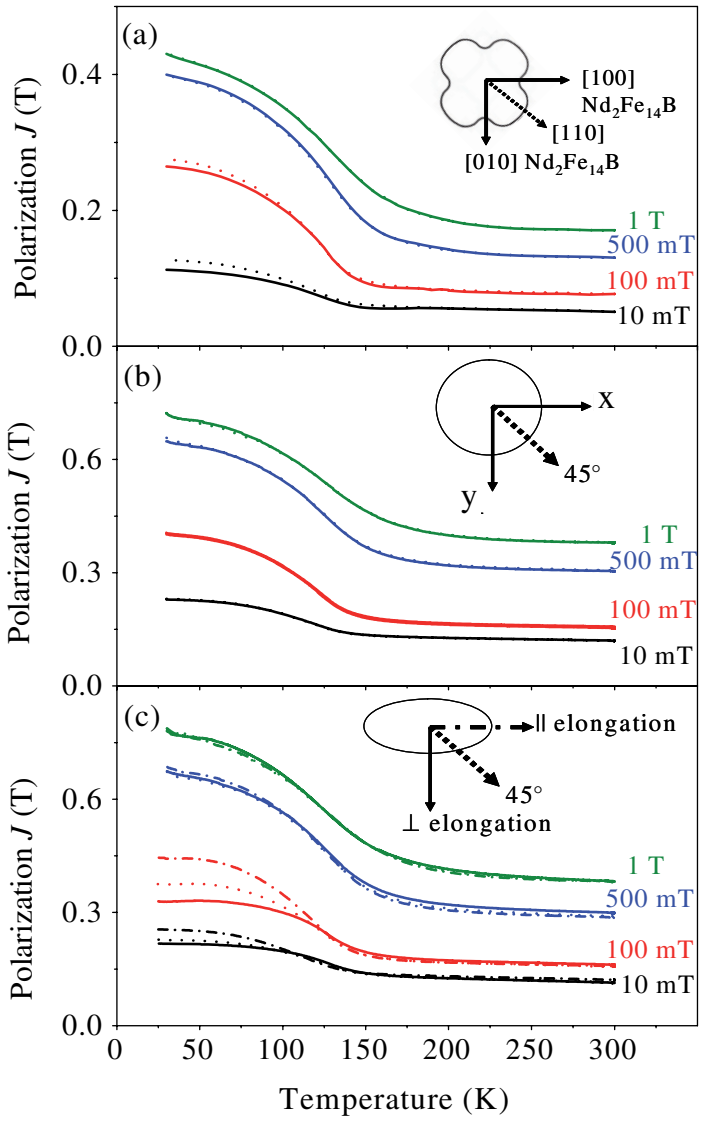

Figure 4. Spin-reorientation transition. Temperature-dependent magnetic polarization J is shown for Nd–Fe–B films grown epitaxially on a combined Cr/Ta buffer on MgO single crystal (a), and grown on Hastelloy in the as-deposited state (b) as well as after 2% elongation of the hastelloy substrate (c). Measurements were made in different in-plane directions and applied fields as marked in the graphs. The sketch in each part illustrates the respective in-plane magnetic anisotropy.

cells in the as-deposited state (30.98 Å^3) is equivalent to the theoretical value of bulk Mo; after elongation (31.08 Å^3) it increases slightly by 0.3%.

3.2. Magnetic properties of Nd–Fe–B films

The consequence of strain on the magnetic properties is examined by temperature-dependent measurements of the magnetic polarization J (figure 4). Films have been saturated at room

temperature perpendicular to the film plane in order to align the maximum moment along the *c*-axis, and then measured with the field applied in key different in-plane directions. For comparison, epitaxial films grown on Cr/Ta [34, 35] with one single orientation have been investigated and are shown in figure 4(a). At temperatures above the spin-reorientation temperature (T_{SR}) of 135 K, the moment measured in plane is low due to the large uniaxial out-of-plane anisotropy. This allows only a small rotation of the magnetization from the easy axis into the field direction. At lower temperatures, the magnetically favored magnetization direction lies on an easy cone toward the crystallographic *c*-axis and the opening angle increases with lower temperature. Hence a certain projection of the magnetization vector contributes also to the in-plane measurement and the in-plane magnetization increases with decreasing temperature. For a perfectly aligned tetragonal crystal, however, not all in-plane directions are identical. As seen by the increased moment along the $[110]_{NdFeB}$ direction compared with the $[100]_{NdFeB}$, the latter direction is favored in agreement with the basal plane anisotropy of the $Nd_2Fe_{14}B$ single crystal [36]. When increasing the applied field to about 500 mT, this in-plane anisotropy is overcome and identical moments are measured for both directions. While films on Cr/Ta buffer layers are discontinuous, a Mo buffer layer results in smooth and continuous Nd–Fe–B films [34], which allow the analysis of strain effects. The three epitaxial orientations of the $Nd_2Fe_{14}B$ films on the IBAD MgO buffer result in an averaging of the fourfold crystal symmetry. Hence, no distinguishable polarization is obtained for measuring along different in-plane orientations as the preferential direction lies on a simple easy cone (figure 4(b)). The applied uniaxial plastic strain breaks the symmetry compared to the as-deposited state. The polarization measured along the elongation direction increases compared with the perpendicular direction, and measurements in the 45° direction as well as in the unstrained state take intermediate values. Comparable to a positive magnetostriction constant, the easy cone of the unstrained state is now deformed to an ellipse (figure 4(c)). In all three cases shown in figure 4, the spin-reorientation temperature T_{SR} is not affected significantly. This indicates that the strain only affects the opening angle during the spin reorientation. As the same samples were measured before and after straining them plastically, any influence of surface/interface anisotropies can be neglected.

4. Summary

The use of a ductile Hastelloy substrate together with an IBAD-textured MgO(001) buffer allows for the growth of an epitaxial film, similar to on a brittle MgO(001) substrate. This ductile substrate has been plastically strained by an external uniaxial load resulting in an anisotropic strain within the film, and hence breaking the in-plane symmetry. By a uniaxial 2% plastic deformation of the substrate, an elastic strain of 0.8% within the Mo buffer is obtained. This strain significantly influences the magnetic properties of the epitaxial $Nd_2Fe_{14}B$ film. An elliptically distorted easy cone is observed below the spin-reorientation temperature, exceeding the in-plane anisotropy of the tetragonal unit cell as measured for a film grown on a MgO(001) single crystal. This proves the principal suitability of our approach to examine the influence of large uniaxial strain on the functional properties of various materials, accessible neither in bulk materials nor in films prepared on rigid substrates. It will allow for a more detailed evaluation of crystal electric field (CEF) models [37] used to describe the intrinsic magnetic properties and especially the anisotropies of these rare-earth transition metal compounds. Although the strain

was limited to 2% for the specific $Nd_2Fe_{14}B$ system, significantly larger strain is applicable for less brittle systems. This will also allow the examination of nonlinear effects.

Acknowledgments

We acknowledge H J Klauß for experimental support and financial support by the DFG as a part of SFB 463: 'Rare earth transition metal compounds: structure, magnetism and transport'.

References

[1] Choi K J *et al* 2004 *Science* **306** 1005
[2] Chen Y, Mei Y, Kaltofen R, Mönch J I, Schumann J, Freudenberger J, Klauß H-J and Schmidt O 2008 *Adv. Mater.* **20** 3224
[3] Rata A D, Herklotz A, Nenkov K, Schultz L and Dörr K 2008 *Phys. Rev. Lett.* **100** 076401
[4] Hühne R, Okai D, Dörr K, Trommler S, Herklotz A, Holzapfel B and Schultz L 2008 *Supercond. Sci. Technol.* **21** 075020
[5] Thomas M, Heczko O, Buschbeck J, Schultz L and Fähler S 2008 *Appl. Phys. Lett.* **92** 192515
[6] Eerenstein W, Mathur N D and Scott J F 2006 *Nature* **442** 759
[7] Mañosa L, Moya X, Planes A, Gutfleisch O, Lubina J, Barrio M, Tamarit J-L, Aksoy S, Krenke T and Acet M 2008 *Appl. Phys. Lett.* **92** 012515
[8] Lyubina J, Nenkov K, Schultz L and Gutfleisch O 2008 *Phys. Rev. Lett.* **101** 177203
[9] Mosca D H, Vidal F and Etgens V H 2008 *Phys. Rev. Lett.* **101** 125503
[10] Bonnot E, Romero R, Mañosa L, Vives E and Planes A 2008 *Phys. Rev. Lett.* **100** 125901
[11] Díaz-Sánchez L E, Romero A H, Cardona M, Kremer R K and Gonze X 2007 *Phys. Rev. Lett.* **99** 165504
[12] Granado E, Eleoterio M S, Garcia-Flores A F, Souza J A, Glolvenchits E I and Sanina V A 2008 *Phys. Rev.* B **77** 134101
[13] Rosner H *et al* 2006 *Nat. Phys.* **2** 469
[14] Mironets O, Meyerheim H L, Tusche C, Stepanyuk V S, Soyka E, Zschack P, Hong H, Jeutter N, Felici R and Kirschner J 2008 *Phys. Rev. Lett.* **100** 096103
[15] Winkelmann A, Przybylski M, Luo F, Shi Y and Barthel J 2006 *Phys. Rev. Lett.* **96** 257205
[16] Huang H and Spaepen F 2000 *Acta Mater.* **48** 3261
[17] Ohring M 2002 *Materials Science of Thin Films: Deposition and Structure* (London: Academic) chapter 12
[18] Huang W, Zhu J, Zeng H Z, Wei X H, Zhan Y and Li Y R 2006 *Appl. Phys. Lett.* **89** 262506
[19] Thiele C, Dörr K, Fähler S, Schultz L, Meyer D C, Levin A A and Paufler P 2005 *Appl. Phys. Lett.* **87** 262502
[20] Mohanan S and Herr U 2007 *J. Appl. Phys.* **102** 093903
[21] Haynes international Inc. http://www.haynesintl.com
[22] Matias V, Hänisch J, John Rowley E and Güth K 2009 *J. Mater. Res.* **24** 125
[23] Kaneko Y 2004 *Proc. 18th Int. Workshop on High Performance Magnets and Their Applications* vol 1 p 40
[24] Serrona L K E B, Sugimura A, Adachi N, Okuda T, Ohsato H, Sakamoto I, Nakamishi A, Motokawa M, Ping D H and Hono K 2003 *Appl. Phys. Lett.* **82** 1751
[25] Araki T, Nakanishi T and Umemura T J 1999 *J. Appl. Phys.* **85** 4877
[26] Castaldi L, Gibbs M R J and Davies H A 2003 *J. Appl. Phys.* **93** 9165
[27] Hannemann U, Fähler S, Neu V, Holzapfel B and Schultz L 2003 *Appl. Phys. Lett.* **82** 3710
[28] Neu V, Melcher S, Hannemann U, Fähler S and Schultz L 2004 *Phys. Rev.* B **70** 144418
[29] Abache C and Oesterreicher J 1986 *J. Appl. Phys.* **60** 3671
[30] Kuz'min M D, Garcia L M, Plaza I, Bartolome J, Fruchart D and Buschow K H J 1995 *J. Magn. Magn. Mater.* **146** 77

[31] Ibarra M R, Algarabei P A, Alerdi A, Batolome J and del Moral A 1987 *J. Appl. Phys.* **61** 3451
[32] Yang N, Dennis K W, McCallum R W, Kramer M J, Zhang Y and Lee P L 2005 *J. Magn. Magn. Mater.* **295** 65
[33] Andreev A V 1995 *Handbook of Magnetic Materials* vol 8 (Amsterdam: Elsevier) chapter 2
[34] Kwon A R, Neu V, Schultz L and Fähler S 2007 *J. Appl. Phys.* **101** 09K506
[35] Kwon A R, Fähler S, Neu V and Schultz L 2006 *J. Magn. Magn. Mater.* **302** 252
[36] Yamada O, Tokuhara J, Ono F, Sagawa M and Matsuura Y 1986 *J. Magn. Magn. Mater.* **54–57** 585
[37] Kato H, Yamada M and Miyazaki T 2004 *J. Magn. Magn. Mater.* **272–276** 2051